31P-nuclear magnetic resonance studies of chronic myocardial ischemia in the Yucatan micropig.

D P Rath, … , R L Hamlin, P M Robitaille

J Clin Invest. 1995;95(1):151-157. https://doi.org/10.1172/JCI117632.

Research Article

In this work, an x-irradiation/high fat/high cholesterol diet-induced atherogenic model was invoked to examine the effects of severe diffuse atherosclerosis on myocardial metabolism in the in vivo porcine heart. This model was studied using spatially localized 31P-nuclear magnetic resonance (NMR) to monitor pH and the levels of inorganic phosphate, phosphomonoesters, creatine phosphate, and adenosine triphosphate as a function of workload transmurally in control swine and in animals suffering from chronic ischemic heart disease. These preliminary studies revealed that the development of severe atherosclerosis and the accompanying chronically diseased state produce changes in high energy phosphates and that increases in rate pressure products result in demonstrable signs of ischemia in the myocardium which span the entire left ventricular wall. Ischemic changes include a global increase in inorganic phosphate and corresponding decreases in creatine phosphate, ATP, and pH. Importantly, changes in intracellular pH are noted with even the slightest increase in workload suggesting that these diseased hearts display elevated glycolytic activity. By challenging these animals with increased cardiac workload, we directly visualize how the chronically compromised heart responds to severe oxygen challenges in a clinically relevant model of this situation.

^{31}P-Nuclear Magnetic Resonance Studies of Chronic Myocardial Ischemia in the Yucatan Micropig

Dipti P. Rath,* Michael Bailey,§ Huzeng Zhang,* Zhongchen Jiang,* Amir M. Abduljalil,* Steven Weisbrode,§ Robert L. Hamlin,‖ and Pierre-Marie L. Robitaille*‡

*Departments of *Radiology, ‡Medical Biochemistry, §Veterinary Clinical Sciences, and ‖Veterinary Physiology and Pharmacology, The Ohio State University, Columbus, Ohio 43210*

Abstract

In this work, an x-irradiation/high fat/high cholesterol diet–induced atherogenic model was invoked to examine the effects of severe diffuse atherosclerosis on myocardial metabolism in the in vivo porcine heart. This model was studied using spatially localized ^{31}P-nuclear magnetic resonance (NMR) to monitor pH and the levels of inorganic phosphate, phosphomonoesters, creatine phosphate, and adenosine triphosphate as a function of workload transmurally in control swine and in animals suffering from chronic ischemic heart disease. These preliminary studies revealed that the development of severe atherosclerosis and the accompanying chronically diseased state produce changes in high energy phosphates and that increases in rate pressure products result in demonstrable signs of ischemia in the myocardium which span the entire left ventricular wall. Ischemic changes include a global increase in inorganic phosphate and corresponding decreases in creatine phosphate, ATP, and pH. Importantly, changes in intracellular pH are noted with even the slightest increase in workload suggesting that these diseased hearts display elevated glycolytic activity. By challenging these animals with increased cardiac workload, we directly visualize how the chronically compromised heart responds to severe oxygen challenges in a clinically relevant model of this situation. (*J. Clin. Invest.* 1995. 95:151–157.) Key words: ischemia • atherosclerosis • myocardium • nuclear magnetic resonance • metabolism

Introduction

The incidences of myocardial infarction and atherosclerosis are mutually intertwined (1). Nonetheless, the victim of coronary insufficiency is likely to experience brief repeated myocardial ischemic episodes brought on by advanced atherosclerosis before actual infarction. Thus, acute myocardial infarction is often a manifestation of the chronic atherosclerotic state. This condition, from a metabolic point of view, is significantly different from acute ischemic injury caused by such conditions as sudden coronary thrombosis or trauma.

Extensive studies have been undertaken to examine the effects of repeated controlled ischemic episodes in the myocardium. These studies have been driven by the concept of myocardial preconditioning (2–7), a hypothesis which advances that the myocardium becomes more resistant to the effects of ischemia as a result of repeated ischemic periods. For instance, ischemic preconditioning has been associated with reduced infarct sizes in the swine (3) and with the absence of cumulative ATP loss in the canine (4, 5). As such, there is a growing body of evidence that a few brief periods of ischemia condition the myocardium and increase its tolerance to longer periods of ischemia (2–7). While the results of these preconditioning studies are interesting, they have limited relevance to the clinical situation. This is because (*a*) these preconditioning studies have arbitrary ischemic episodes whose duration and frequencies are determined nonphysiologically; (*b*) these studies are conducted in such a way as to provide insufficient time for gene expression and protein synthesis (the real makers of adaptation); (*c*) these studies cannot easily mimic the gradual onset of atherosclerosis; and (*d*) most interestingly in terms of clinical relevance, the duration of such protective effects appears to be transient (8, 9).

In this work, we use spatially localized ^{31}P-nuclear magnetic resonance (NMR)[1] to examine a swine model of ischemic heart disease that is based on the same pathology (atherosclerosis) observed in humans. Atherogenesis has been extensively studied in the swine (10–15), and aged swine display spontaneous atherosclerotic lesions which very closely resemble the pathological situation found in humans (10–14). Indeed swine appear to be particularly susceptible to this disease as reflected by the fact that atherosclerosis can be detected in all examinations of swine over 1 yr of age under normal diet conditions (11). Interestingly in the swine, lesions occur in a regionally specific fashion with pathological changes occurring preferentially at some locations, while others are always devoid of lesions (11). These features, when coupled with the fact that the swine is an omnivore closely resembling man in its diet, strongly support the use of this species in studies of atherogenesis. In addition, the swine's cardiovascular system provides an excellent model of the human condition in terms of lipoprotein structures, size, and vasculature (16, 17). Thus, the swine is clearly a model of choice for studies of chronic ischemia resulting from atherosclerosis.

Unfortunately, while the pathology of atherosclerosis in the swine closely mimics that which is observed in humans, this condition develops at an extremely slow pace. As a result, experimental models of atherosclerosis which are primarily based

Address correspondence to Pierre-Marie Robataille, PhD, MRI Facility, 1630 Upham Drive, Ohio State University Hospitals, Columbus, OH 43210.

Received for publication 13 January 1994 and in revised form 25 April 1994.

J. Clin. Invest.

0021-9738/95/01/0151/07 $2.00
Volume 95, January 1995, 151–157

1. *Abbreviations used in this paper:* LAD, left anterior descending coronary artery; NMR, nuclear magnetic resonance; P_i, inorganic phosphate; RPP, rate pressure product.

on high fat/high cholesterol diets have been developed and all strains of swine studied with this approach have demonstrated an accelerated development of lesions (15). In addition, the number and severity of the lesions increased with these hyperlipidemic diets (15). These lesions appear to arise primarily from increases in intimal cell masses which are primarily comprised of lipid-rich calcific necrotic debris (12, 13). While these results with hyperlipidemic diets reduce the time of onset to experimental atherosclerosis, these models are not yet suitable for the study of chronic ischemia. This is because the lesions that develop under these conditions are not severe enough to result in the chronic myocardial ischemia, myocardial infarction, and occasional sudden death that are associated with human vascular disease (18). However, these features, associated with severe atherosclerosis, can be produced in experimental swine models by injuring the endothelial layer of the artery using either a balloon catheter (18) or x irradiation (19). Application of these methods further accelerates the time of atherogenesis onset and ensures an endpoint that closely mimics the most severe human disease (12). In many cases, myocardial infarction occurs within 2–3 mo (18, 19).

As such, in this work we provide a qualitative and quantitative NMR analysis of the chronically ischemic myocardium in an attempt to understand both the true end points of ischemic heart disease and the cellular adaptations to this condition using the x irradiation and high cholesterol model proposed by Lee et al. (19). Our decision to use this particular model was based in part on the extreme difficulties anticipated in implementing balloon catheter methods proposed by Lee and Lee (18) in a 2-wk-old micropig, and similar difficulties associated with placing an ameroid constrictor around the left anterior descending coronary artery (LAD) of such a small animal.

Methods

Preparation of micropigs with coronary atherosclerosis. Animals were prepared following the general procedure previously outlined by Lee et al. (19). Briefly, however, upon receipt from the vendor, weanling, male Yucatan micropigs were adapted to their new environment for 1 wk, and fed commercial mash for weanlings. On day 1 of week 2, some of the pigs received half commercial mash and half hypercholesterolemic diet, and each succeeding day of that week they received more hypercholesterolemic diet and less commercial mash; until, by day 1 of week 3, they received only hypercholesterolemic diet. The remaining animals stayed on standard commercial mash. Serum cholesterol levels were monitored by sampling the cranial vena cava after 2 wk and 7 wk on the diet. At the end of 2 wk all animals were anesthetized with a mixture of ketamine (10 mg/kg) and diazepam (0.25 mg/kg), given intramuscularly, followed in 15 min by inhalation of 1% halothane in oxygen. All pigs were then placed for 5 min in left lateral, and for 5 min in right lateral recumbency, and their thoraces were exposed to a total of 100 rads/kg of x ray from a Cs source. The exposure was collimated to the heart. The animals were then permitted to recover, and this procedure was repeated during weeks 6 and 10 of the period of preparation. In addition to the x-irradiated controls, we also examined nonirradiated controls on normal diets.

In vivo NMR studies. All NMR measurements were performed on an Omega 4.7 T/40 cm spectrometer (GE, Freemont, CA) equipped with actively shielded 26-cm gradients ($\sim$ 5.6 G/cm). After 3–4 mo of preparation, the animal was pre-anesthetized with ketamine, anesthetized 1% halothane in oxygen, and the chest was opened at the fifth intercostal space through a left hemithoracotamy as previously described (20, 21). The heart was then suspended in a pericardial cradle and a 3-mm o.d., 100-cm polyvinylchloride (PVC) catheter filled with heparin saline solution was introduced into the left ventricle through the apical dimple and secured with a purse-string suture. This catheter was connected to a disposable transducer and was used to monitor intraventricular pressure. For these studies, a 22-mm single turn surface coil made of silver wire (AWG 16) was sutured onto the left ventricle over the region perfused by the LAD. The surface coil was thus placed over myocardium nourished by obviously atherosclerotic arteries. Before suturing the surface coil onto the myocardium, a polyvinylchloride capillary containing 15 μl of 3 M phosphonoacetate was permanently positioned in the plane of the coil. This capillary was used to determine the 90° pulse (20, 21) at the center of the coil and to set the position of the voxels for the FLAX-ISIS experiment (20, 21). Once the surgical preparation was completed, the animal was positioned in the isocenter of the magnet (20). The homogeneity of the magnetic field was adjusted by applying an adiabatic half passage pulse (20, 22) in the presence of cardiac gating (23). The respiration was gated to the cardiac cycle of the animal and to NMR acquisition as previously described by this laboratory (23). Data was acquired in diastole by also gating the spectrometer to the cardiac cycle (23). ^{31}P-NMR data were then acquired with 12-s repetition times (24) using a single adiabatic half passage experiment (22) or using the FLAX-ISIS technique described previously (20, 21). With this approach, a complete transmural data set was acquired in $\sim$ 25 min. NMR spectra were acquired at basal rate pressure products and following a change to high workloads. The workloads were altered by intravenous infusion of dobutamine hydrochloride (Eli Lilly and Co., Indianapolis, IN). During all NMR studies, arterial blood samples (5 ml) were withdrawn every half hour and the pH, CO_2, and O_2 levels evaluated using an IL 1302 blood gas analyzer (Ilford Ltd., Basildon, Essex, UK). At the end of each study the animal was killed using sodium pentobarbital (160 mg/kg). NMR spectra were then integrated using standard GE Omega software (General Electric Co., Milwaukee, WI). Internal consistency, both transmurally and as a function of changing rate pressure products, was ensured by integrating all resonances relative to the area of the creatine phosphate observed in the endocardial voxel at the lowest workload.

Histology. Some animals were subjected to histological analysis to quantify the extent of atherosclerosis and myocardial injury. To obtain histological results, the hearts were quickly removed while the pigs were still fully anesthetized. The coronary circulation was then perfused with iced saline and then with 10% buffered formalin. Hearts were fixed for 4 d in 10% buffered formalin, and breadloaf sections 5 mm thick were cut from apex to base using a commercial bacon slicer. Myocardium was stained with hemotoxylin and eosin, Masson's trichrome for fibrous connective tissue, and von Kossa for mineralization. Coronary arteries were stained with hemotoxylin and eosin. Myocardium was analyzed for the presence of areas of mineralization and nuclear hypertrophy and for regions of myocardial necrosis. Coronary arteries were analyzed for degree of stenosis and to document the extent of atherosclerotic lesions in the coronary bed. The myocardium beneath the region analyzed by NMR and the coronary arteries perfusing this region were examined in greatest depth. A total of 11 diseased animals were analysed histologically, while only nine of these animals were analyzed by NMR.

Results

After feeding pigs the hypercholesterolemic diet for 2 wk, serum cholesterol averaged 1200±170 mg/dl and dropped by the seventh week to 510±130 mg/dl. Electrocardiogram recordings were unremarkable. Histological exams revealed normal myocardial tissue for all normal and x-irradiated controls, although mild neutrophilic vasculitis was found in the LAD and diagonal branch in the x-irradiated controls (Fig. 1 *A*). This mild neutrophilic vasculitis was a likely result of radiation injury as expected. Myocardial tissue in these animals was normal to light microscopic examination. In sharp contrast, mild to severe atherosclerosis was found in the LAD and diagonal branch of all

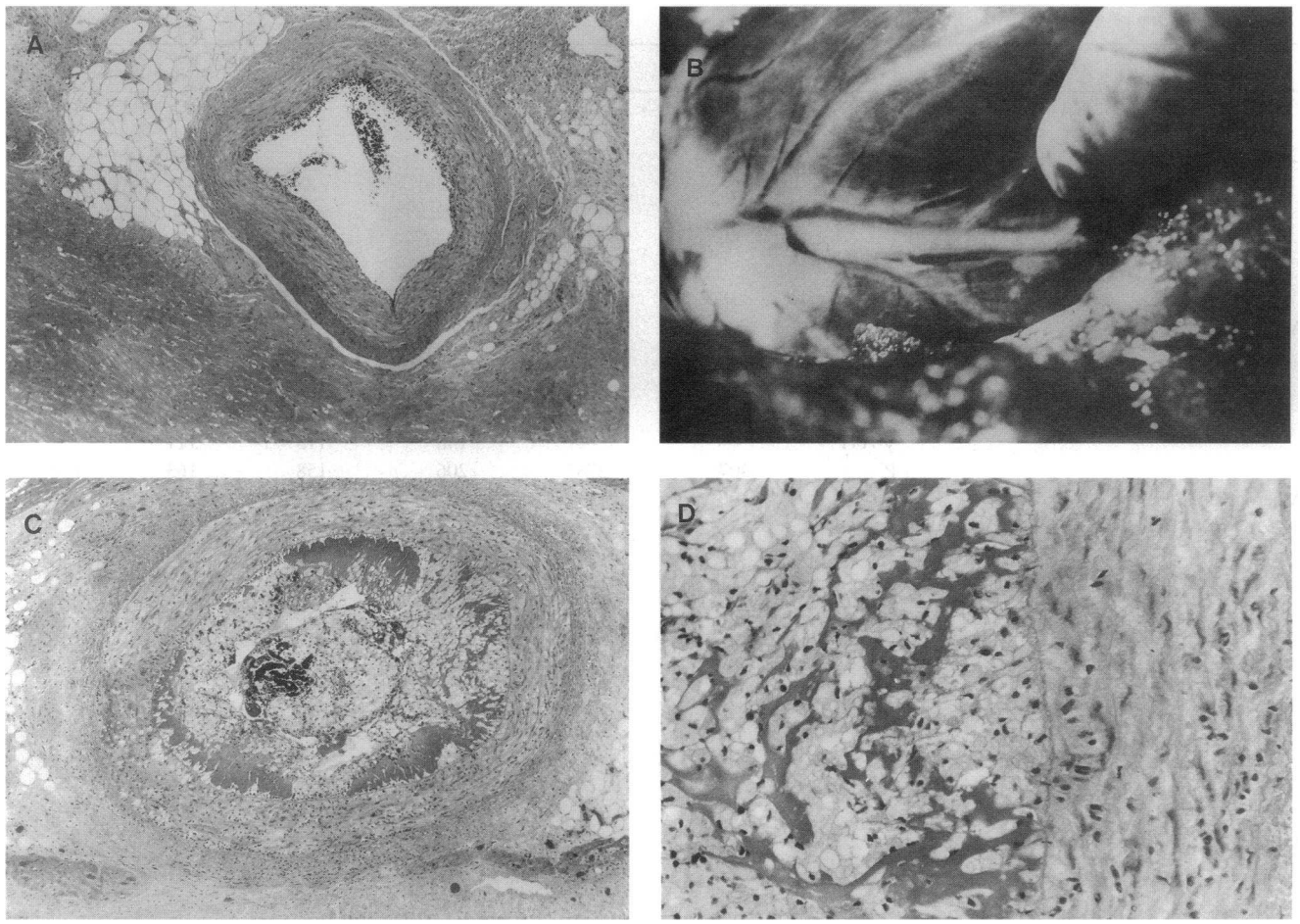

Figure 1. (*A*) Neutrophilic vasculitis in an x-irradiated control pig demonstrating, at this magnification, a dense hypercellular subintimal infiltrate with disruption of the intima. The lesion is restricted to a portion of the vessel. Myocardial lesions were not detected in these animals. (*B*) Photograph of the left ventricle from a pig placed on a high cholesterol diet. Note the severe atherosclerosis in the LAD of this animal. (*C*) Light microscopic display of atherosclerosis in an animal placed on a high cholesterol diet. The subintima is thickened with numerous foamy macrophages. The lesion in this focus is pronounced. (*D*) Higher magnification of Fig. 1 *C*, confirming the foamy nature of the macrophages that are admixed with hemorrhage and plasma. The lumen of the vessel is markedly compromised by still patent and visible as crescentic endothelial-lined slits.

(11/11) pigs on the high cholesterol diet (Fig. 1, *B, C,* and *D*). Pigs on the high cholesterol diets also showed multifocal areas of mineralization, light and scattered nuclear hypertrophy, and regions of myocardial necrosis compatible with response to ischemia and associated with pronounced atherosclerotic lesions in the coronary bed. Control animals lacked all signs of lesion formation.

Transmural NMR data from control micropigs and from atherogenic animals have been summarized in Table I. Transmural ^{31}P-NMR spectra obtained from x-irradiated control micropigs ($n = 3$) on a normal diet were indistinguishable from those of normal control pigs ($n = 7$) and are summarized as one group in Table I. A representative set of spectra from x-irradiated an x-irradiated control at low workload is shown in Fig. 2 *A*. In this series of figures, spectra corresponding to the epicardial region of the myocardium are displayed at the top of the figure (the endocardial file is the lowermost). Note, the absence of elevated inorganic phosphate in all myocardial layers for this x-irradiated animal. From the chemical shift of the inorganic phosphate resonance in these spectra a global intramyocardial pH of 7.0±0.05 could be calculated. In calculating this value, however, we urge some caution and note the poor signal to noise of the inorganic phosphate resonance used to derive the parameter. In contrast, transmural ^{31}P-NMR spectra obtained from an animal with severe atherosclerosis (animal 1 in Table I) is shown in Fig. 2 *B*. Note the pronounced elevation of inorganic phosphate in the epicardial files and the absence of high energy phosphate in the endocardial region for this animal. These spectra reveal a slightly lowered epicardial intracellular pH of 6.84±0.05, as noted by analyzing the inorganic phosphate chemical shift. These spectra were acquired with a 22-mm surface coil and this animal had a 1.1-cm thick wall under the region sampled by the coil. As a result, the innermost files are truly endocardial and do not correspond to 2,3-diphosphoglycenic acid in the left ventricle (20, 21, 25). We have yet to establish the nature of the phosphomonoesters in such spectra, however, they may be associated with hibernating myocardium in these chronically ischemic hearts. The rate pressure product in this animal could not be substantially elevated (5,000 to 7,000 mmHg/min).

Fig. 3 displays transmural ^{31}P-NMR spectra obtained from a normal control pig (Fig. 3, *A* and *B*) and from two chronically

Table I. Summary of ^{31}P-NMR Spectra

	RPP		Endo	Endo-mid	Mid	Mid-epi	Epi	Global‡ P_i
	mmHg/min							
Controls	6000±1010	CP	100	109	117	161	170	
		γ-ATP	60	50	62	87	74	
		P_i	36	20	19	25	24	23
	14770±840	CP	99	109	125	136	130	
		γ-ATP	57	52	51	63	81	
		P_i	38	20	24	22	29	25
Atherogenic 1	5000	CP	—	—	210	283	240	
		γ-ATP	—	—	162	115	116	
		P_i	398*	301*	192	155	155	167
	7000	CP	—	—	228	291	196	
		γ-ATP	—	—	148	115	111	
		P_i	407*	278*	206	158	163	176
Atherogenic 2	6750	CP	100	171	154	169	140	
		γ-ATP	51	53	58	45	58	
		P_i	92*	50*	44	60	54	53
	8770	CP	61	103	157	130	114	
		γ-ATP	33	42	48	50	29	
		P_i	181*	83	61	144	115	107
Atherogenic 3	6480	CP	100	100	81	93	105	
		γ-ATP	50	52	35	37	43	
		P_i	16	17	19	41	33	31
	18000	CP	57	65	77	102	117	
		γ-ATP	20	24	20	34	37	
		P_i	67	36	71	75	30	59
Atherogenic 4	7300	CP	100	90	123	155	127	
		γ-ATP	49	44	47	57	41	
		P_i	219*	137*	106*	48	21	58*
	13200	CP	79	86	107	129	99	
		γ-ATP	44	34	41	54	46	
		P_i	250*	160*	79*	72	27	59*
Atherogenic 5	8640	CP	100	90	158	185	209	
		γ-ATP	75	44	82	98	83	
		P_i	48	36	31	82	68	60
	15900	CP	95	48	70	91	71	
		γ-ATP	—	30	40	60	51	
		P_i	—	55	72	98	107	92
Atherogenic 6	6050	CP	100	130	166	157	165	
		γ-ATP	59	66	66	63	36	
		P_i	152*	88*	29	45	48	41
	12960	CP	—	87	96	185	171	
		γ-ATP	—	—	51	33	27	
		P_i	311*	257*	184	170	175	176
Atherogenic 7	6350	CP	—	167	253	246	226	
		γ-ATP	—	99	87	108	129	
		P_i	321*	222*	20	24	20	21
	11000	CP	—	200	222	231	209	
		γ-ATP	—	116	113	105	113	
		P_i	297*	204*	88	51	83	74
Atherogenic 8	5580	CP	100	150	214	200	196	
		γ-ATP	—	78	50	54	43	
		P_i	451*	214*	70	220	242	177
Atherogenic 9	6720	CP	100	93	74	79	46	
		γ-ATP	50	39	35	31	17	
		P_i	110*	101*	41	63	65	56
	13050	CP	105	67	42	—	—	
		γ-ATP	44	41	23	—	—	
		P_i	175*	161	140	173	170	161

Table I. (Continued)

	RPP		Endo	Endo-mid	Mid	Mid-epi	Epi	Global‡ P_i
Atherogenics§	6450±1070	CP	100	129	164	176	166	
		γ-ATP	57	61	72	69	66	
		P_i	199	129	55	86	85	76‖
	12380±3840	CP	79	95	128	172	147	
		γ-ATP	32	51	64	66	61	
		P_i	240	153	118	125	121	121¶**

* Integral reflects some overlap with phosphomonoesters and 2,3-DPG. ‡ Endo and endo-mid layers are excluded to avoid contamination from PME and 2,3-DPG. § Atherogenic 4 is excluded in computing averages. Please see text. ‖ Significantly different from control ($P = 0.0003$). ¶ Significantly different from control ($P < 0.0001$). ** Significantly different from low workload ($P = 0.013$). CP, creatine phosphate; PME, phosphomonoesters.

ischemic animals (Fig. 3, *C–F*; animals 2 and 3 in Table I) at both low (Fig. 3, *A, C,* and *E*) and elevated (Fig. 3, *B, D,* and *F*) rate pressure products. In agreement with previous observation in the canine (21), no significant changes were observed in the spectra of control micropigs in response to increases in rate pressure products (Fig. 3, *A* and *B*). In this control animal,

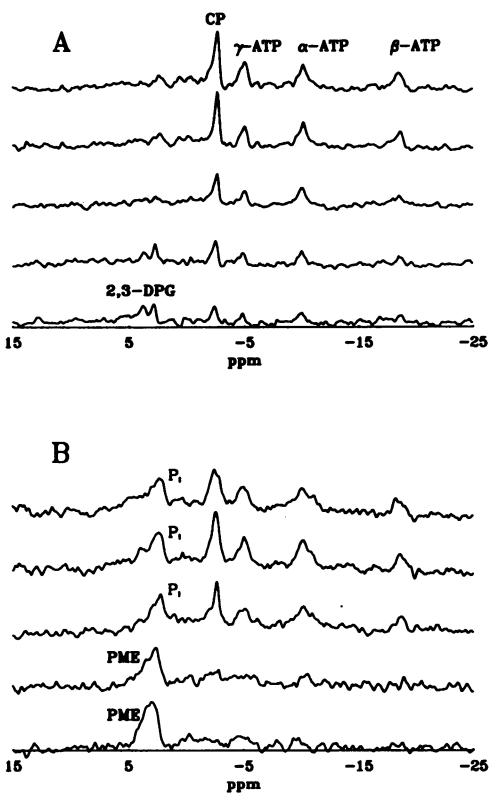

Figure 2. Transmural ^{31}P-NMR spectra acquired from an x-irradiated control micropig (*A*, RPP = 5,000 mmHg/min) and from an x-irradiated micropig previously placed on a high fat/cholesterol diet (*B*, RPP = 5,000 mmHg/min). Resonances corresponding to creatine phosphate (CP), ATP, 2,3-diphosphoglyceric acid (2,3-DPG), P_i, and phosphomonoesters (PME). Note the increased phosphomonoesters and the pronounced loss of high energy phosphates in the endocardial lamina of the diseased animal (see text). These spectra were obtain at basal rate pressure products and are displayed with the epicardial lamina at the top of the figure and the endocardial lamina at the bottom.

inorganic phosphate levels were too low to enable the determination of intracellular pH. Without exception, all micropigs on high cholesterol diets that had significant atherosclerosis on histological examination had globally elevated inorganic phosphate even at the lowest rate pressure product (RPP) relative to the control animals (see Table I). This is displayed clearly in Fig. 3, *C* and *E* (compare with Figs. 2 *A* and 3 *A*). One micropig on the high cholesterol diet which did not develop pronounced atherosclerotic lesions looked essentially like an x-irradiated control (animal 4 in Table I). Note in particular the low inorganic phosphate (P_i) levels in this animal even at elevated workloads. Elevation of RPP in diseased animals with dobutamine resulted in a global increase in inorganic phosphate accompanied by an immediate decrease in intracellular pH, creatine phosphate, and ATP (Fig. 3, *C–F*). Specifically, intracellular pH values dropped from a global average of 7.0±0.1 to 6.78±0.05 and from 6.92±0.05 to 6.80±0.05 in Fig. 3, *C,* and *D* (animal 2) and Fig. 3, *E* and *F* (animal 3), respectively. More dramatic results are displayed in Fig. 4, *A–D* and the generality of these conclusions is clearly evident in the summary data for the diseased animals provided in Table I. As shown in these spectra, increases in rate pressure products in these animals resulted in severe depletion of both creatine phosphate and ATP along with a complementary expected increase in P_i. In Fig. 4, *A* and *B* (animal 5) global intracellular pH values fell from 7.05±0.05 to 6.80±0.05 as a result of dobutamine infusion. The animal shown in Fig. 4, *C* and *D* (animal 6) displayed the highest resting intracellular inorganic phosphate levels and revealed a reduced global intracellular pH value of 6.75±0.05 even at the lowest workload. This animal experienced no measurable change in intracellular pH on raising the rate pressure product. Interestingly, this was the case even though the myocardium experienced substantial changes in high energy phosphate levels. No significant transmural variation in intracellular pH values was noted in these animals. Histological analysis revealed no signs of infarction in these hearts although these results point to pronounced biochemical changes in these animals.

Discussion

The global increase in P_i in the severely atherosclerotic animals and the simultaneous shift in pH from normal values observed in increasing rate pressure products under our conditions is contrary to an acute canine model of graded ischemia (25, 26,

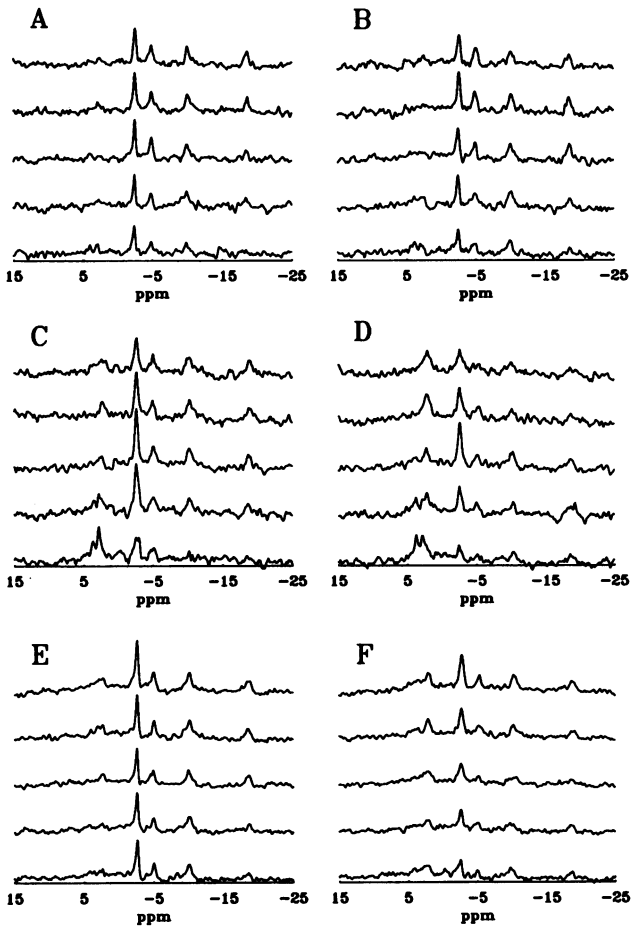

Figure 3. Transmural ^{31}P-NMR spectra acquired from a control micropig (*A, B*) and from x-irradiated micropigs previously placed on high fat/cholesterol diet (*C–F*). Results were obtained at basal (*A,* RPP = 6,900 mmHg/min; *C,* RPP = 6,800 mmHg/min; *E,* RPP = 6,500 mmHg/min) and elevated (*B,* RPP = 13,100 mmHg/min; *D,* RPP = 8,700 mmHg/min; *F,* RPP = 18,000 mmHg/min) rate pressure products. Note that even a very slight increase in rate pressure products for the animal displayed in *C* and *D* resulted in a pronounced change in high energy phosphates accompanied with a 0.2 unit drop in global intracellular pH.

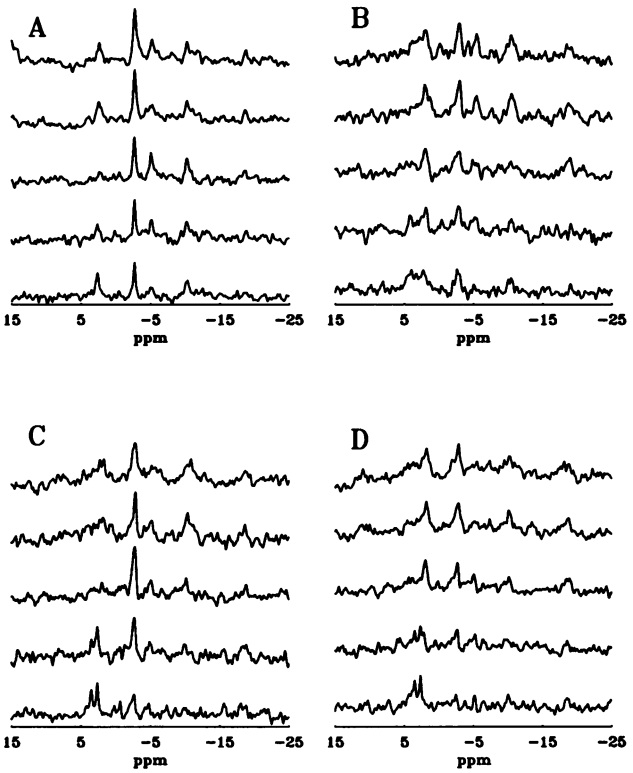

Figure 4. Transmural ^{31}P-NMR spectra acquired from two x-irradiated micropigs previously placed on high fat/cholesterol diet. Results were obtained at basal (*A,* RPP = 8,600 mmHg/min; *C,* RPP = 6,100 mmHg/min) and elevated (*B,* RPP = 15,900 mmHg/min; *D,* RPP = 13,000 mmHg/min) rate pressure products. Note the elevation of inorganic phosphate in these spectra even at basal rate pressure products. Interestingly, the animal displayed in *C* and *D* had a decreased global intracellular pH value even at basal rate pressure products and this value did not change appreciably with increased work even though substantial changes are evident in the high energy phosphate profile (see text).

27). In the acute models (25, 26, 27), coronary stenosis resulted in transmurally nonuniform ischemia with inorganic phosphate increasing first in the endocardium without immediate pH changes. These results point to significant differences between acute and chronic models of ischemia and suggest important consequences of myocardial adaptation. For instance, in previous ^{31}P-NMR studies of graded regional ischemia (26), partial stenosis of the LAD with a hydraulic occluder resulted in a decrease in creatine phosphate and ATP along with the complementary increase in P_i in a manner that is closely correlated with changes in blood flow. These changes take place first in the endocardium and then move as a wavefront towards the epicardium as the severity of the injury increased. Moreover, while the endocardium displayed an increase in P_i in response to progressively severe occlusion, no change in intracellular pH accompanied this increase. This is in sharp contrast to results obtained in this atherogenic model, where ischemic insults are generally translated into a global attack on the myocardium with little or no transmural differentiation and a significant simultaneous global drop in intracellular pH. It is also interesting that the animal with the highest levels of inorganic phosphate at basal rate pressure products in this study (Fig. 4 *C* and *D*), had an initially decreased global intracellular pH value which did not further decline on increasing workload.

As such, substantial reevaluation of acutely ischemic models of disease may be in order. This is particularly true since models with no previous history of disease directly affect only a very small fraction of the patient population. In addition, the chronically ischemic myocardium seems to respond to oxygen supply and demand imbalances by significantly altered mechanisms, relative to the normal heart, when presented with an "acute ischemic" event. These adaptations on behalf of the chronically ischemic myocardium are likely to affect both the biochemical and physiological functions.

We have also presented preliminary data on the use of the x-irradiation/high fat/high cholesterol porcine atherogenic model as a potentially useful system to evaluate the biochemical changes associated with chronic ischemic adaption in the myocardium. While it is certain that no pathologic model can entirely duplicate the human condition, we believe that this model has several important features that make it attractive for NMR studies of chronic ischemia in particular. These include the

simplicity of the preparation and the severity of the disease, in an animal large enough to enable transmural analysis of its left ventricular wall by NMR methods. Alternative methods such as the use of a balloon catheter to damage the endothelial lining of a particular vessel, or the implantation of an ameroid constrictor are less attractive since they require extensive intervention in very small animals, namely a 2-wk-old micropig. Nonetheless, these models do not invoke potentially harmful x irradiation, and in contrast to the model we have adapted, do not require the use of double controls. While results from x-irradiated controls and normal controls are encouraging, this study suffers from the lack of more x-irradiated controls to absolutely rule out damage from x-irradiation. However, while this work reports only initial findings, the results with diseased animals in this study are drastically different from previous studies invoking acute ischemic injury. Nonetheless, these findings clearly point to the need for further study of this interesting model.

Acknowledgments

We would like to thank Professor Donald Fry for his insightful comments on animal models of atherosclerosis.

This work was supported by a grant from the American Heart Association—Ohio Affiliate (C-90-33).

References

1. American Heart Association. 1988. 1988 Heart Facts. American Heart Association National Center, Dallas, TX.

2. Swain, J. L., R. L. Sabina, J. J. Hines, J. C. Greenfield, and E. W. Holmes. 1984. Repetitive episodes of brief ischemia (12 min) do not produce a cumulative depletion of high energy phosphate compounds. *Cardiovasc. Res.* 18:264–269.

3. Schott, R., S. Rohmann, E. Braun, B. Winkler, S. Jurgens, and W. Schaper. 1989. The effect of ischemic preconditioning on myocardial oxygen consumption (MVO_2) and infarct size in pigs. *J. Mol. Cell. Cardiol.* 21(Suppl. II):482.

4. Reimer, K. A., C. E. Murry, I. Yamasawa, M. L. Hill, and R. B. Jennings. 1986. Four brief periods of myocardial ischemia cause no cumulative ATP loss or necrosis. *Am. J. Physiol.* 251:H1306–1315.

5. Lange, R., J. S. Ingwall, S. L. Hale, K. J. Alker, and R. A. Kloner. 1984. Effects of recurrent ischemia on myocardial high energy phosphate content in canine hearts. *Basic Res. Cardiol.* 79:469–478.

6. Murry, C. E., R. B. Jennings, and K. A. Reimer. 1988. Preconditioning with ischemia: a delay of lethal cell injury in ischemic myocardium. *Basic Res. Cardiol.* 83:550–559.

7. Hoffmeister, H. M., M. Mauser, and W. Schaper. 1982. Repeated short periods of regional myocardial ischemia: effect on local function and high energy phosphate levels. *Basic Res. Cardiol.* 81:361–372.

8. Cohen, M. V., X.-M. Yang, and J. Downey. 1993. Multiple brief episodes of myocardial ischemia abolish protection of ischemic preconditioning seen after 1 episode of brief ischemia. *Circulation.* 88(Suppl. 4-II):733.

9. Li, Y., and R. A. Kloner. 1993. The beneficial effects of preconditioning can be recaptured after they are lost. *Circulation.* 88(Suppl. 4-II):734.

10. Luginbuhl, H., and J. E. T. Jones. 1965. The morphology of spontaneous atherosclerotic lesions in aged swine. *In* Comparative Atherosclerosis. The Morphology of Spontaneous and Induced Atherosclerotic Lesions in Animals and Its Relation to Human Disease. J. C. Roberts, Jr. and R. Straus, editors. Harper & Row, New York. 3–10.

11. Getty, R. 1965. The gross and microscopic occurrence and distribution of spontaneous atherosclerosis in the arteries of swine. *In* Comparative Atherosclerosis. The Morphology of Spontaneous and Induced Atherosclerotic Lesions in Animals and Its Relation to Human Disease. J. C. Roberts, Jr. and R. Straus, editors. Harper & Row, New York. 11–20.

12. Lee, K. T., D. N. Kim, and W. A. Thomas. 1986. Atherosclerosis in Swine. *In* Swine in Cardiovascular Research. H. C. Stanton and H. J. Mersmann, editors. CRC Press, Boca Raton, FL.

13. French, J. E., and M. A. Jennings. 1965. The tunica intima of arteries of swine. *In* Comparative Atherosclerosis. The Morphology of Spontaneous and Induced Atherosclerotic Lesions in Animals and Its Relation to Human Disease. J. C. Roberts, Jr. and R. Straus, editors. Harper & Row, New York. 25–36.

14. Zugibe, F. 1965. Atherosclerosis in the miniature pig. *In* Comparative Atherosclerosis. The Morphology of Spontaneous and Induced Atherosclerotic Lesions in Animals and Its Relation to Human Disease. J. C. Roberts, Jr. and R. Straus, editors. Harper & Row, New York. 37–42.

15. Moreland, A. F. 1965. Experimental atherosclerosis of swine. *In* Comparative Atherosclerosis. The Morphology of Spontaneous and Induced Atherosclerotic Lesions in Animals and Its Relation to Human Disease. J. C. Roberts, Jr. and R. Straus, editors. Harper & Row, New York. 21–24.

16. Stanton, H. C., and H. J. Mersmann. 1986. Swine in Cardiovascular Research. CRC Press, Boca Raton, FL.

17. Bloor, C. M., F. C. White, B. D. Guth, and C. M. Bloor. 1986. Cardiac ischemia and coronary bed flow in swine. *In* Swine in Cardiovascular Research. H. C. Stanton and H. J. Mersmann, editors. CRC Press, Boca Raton, FL.

18. Lee, W. M., and K. T. Lee. 1975. Advanced coronary atherosclerosis in swine produced by combination of balloon-catheter injury and cholesterol feeding. *Exp. Mol. Pathol.* 23:491–499.

19. Lee, K. T., J. Jarmolych, D. N. Kim, C. Grant, J. A. Krasney, W. A. Thomas, and A. M. Bruno. 1971. Production of advanced coronary atherosclerosis, myocardial infarction and "sudden death" in swine. *Exp. Mol. Pathol.* 15:170–190.

20. Robitaille, P.-M., H. Merkle, E. Sublett, K. Hendrich, B. Lew, G. Path, A. H. L. From, R. J. Bache, M. Garwood, and K. Ugurbil. 1989. Spectroscopic imaging and spatial localization using adiabatic pulses and applications to detect transmural metabolite distribution in the canine heart. *Magn. Reson. Med.* 10:14–37.

21. Robitaille, P.-M. L., H. Merkle, B. Lew, G. Path, K. Hendrich, P. Lindstrom, A. H. L. From, M. Garwood, R. J. Bache, and K. Ugurbil. 1990. Transmural high energy phosphate distribution and response to alterations in workload in the normal canine myocardium as studied with spatially localized ^{31}P NMR spectroscopy. *Magn. Reson. Med.* 16:91–116.

22. Bendal, M. R., and D. T. Pegg. 1986. Uniform sample excitation with surface coils for in vivo spectroscopy by adiabatic rapid half passage. *J. Magn. Reson.* 67:376–381.

23. Pruski, J. C., A. Abduljalil, and P.-M. L. Robitaille. 1992. Improved cardiac gating and ventilation timing in animal experiments. *Magn. Reson. Med.* 27:329–337.

24. Rath, D. P., A. M. Abduljalil, and P.-M. L. Robitaille. 1993. Spatially localized ^{31}P NMR measurements of longitudinal relaxation rates in the canine myocardium. *Magn. Reson. Med.* 29:822–825.

25. Path, G., P.-M. L. Robitaille, H. Merkle, M. Tristani, J. Zhang, M. Garwood, A. H. L. From, R. J. Bache, and K. Ugurbil. 1990. Correlation between transmural high energy phosphate levels and myocardial blood flow in the presence of graded coronary stenosis. *Circ. Res.* 67:660–673.

26. Ugurbil, K., H. Merkle, P.-M. L. Robitaille, K. Hendrich, M. Yoshiyama, G. Path, J. Zhang, M. Tristani, A. H. L. From, R. J. Bache, and M. Garwood. 1989. Transmurally heterogeneous myocardial ischemia studied by spatially localized ^{31}P NMR Spectroscopy. *NMR Biomed.* 2:317–328.

27. Gober, J., S. Schaefer, A. Camacho, M. DeGroot, R. Obregon, E. Botvinick, M. Weiner, and B. B. Massie. 1990. Epicardial and endocardial localized ^{31}P magnetic resonance spectroscopy: evidence for metabolic heterogeneity during regional ischemia. *Magn. Reson. Med.* 13:204–215.